J|A|C|S
ARTICLES
Published on Web 09/30/2005

Enhanced Fluorescence from Arrays of Nanoholes in a Gold Film

Alexandre G. Brolo,*,† Shing C. Kwok,† Matthew G. Moffitt,† Reuven Gordon,‡ Jason Riordon,§ and Karen L. Kavanagh§

Contribution from the Department of Chemistry, University of Victoria, P.O. Box 3065, Victoria, B.C., Canada, V8W 3V6, Department of Electrical and Computer Engineering, University of Victoria, P.O. Box 3055, Victoria, B.C., Canada, V8W 3P6, and Department of Physics, Simon Fraser University, 8888 University Drive, Burnaby, B.C., Canada, V5A 1S6

Received July 20, 2005; E-mail: agbrolo@uvic.ca

Abstract: Arrays of sub-wavelength holes (nanoholes) in gold films were used as a substrate for enhanced fluorescence spectroscopy. Seven arrays of nanoholes with distinct periodicities (distances between the holes) were fabricated. The arrays were then spin-coated with polystyrene films containing different concentrations of the fluorescent dye oxazine 720. The dye was excited via resonant extraordinary transmission of the laser source through the nanoholes. Enhanced fluorescence was observed when the geometric characteristics of the arrays allowed for an enhancement in the transmitted excitation. This enhancement occurred via surface plasmon excitation by the laser and a consequential increase in the local electromagnetic field in a sub-wavelength region at the metal−film interface. It was demonstrated that the sensitivity of the fluorescence measurement (change in signal vs change in dye concentration in the polymer film) is significantly larger at the surface plasmon resonance conditions than that obtained from equivalent films on glass substrates. Enhancement factors for the fluorescence emission were calculated for each array, with a maximum enhancement of close to 2 orders of magnitude as compared to the emission of films on glass. The results presented here indicate that arrays of nanoholes are interesting substrates for the development of fluorescence sensors based on surface plasmon resonance, as they provide a platform that allows both spatial confinement and enhancement of excitation light. Moreover, the collinear characteristics of the present optical setup, due to the resonant extraordinary transmission through the nanohole arrays, are more conducive to miniaturization and chip integration than more traditional experimental geometries.

Introduction

Surface plasmons (SPs) are collective electronic oscillations that can be excited in free-electron metallic nanostructures (Cu, Ag, Au) using visible radiation.[1] SP-based analytical methods and spectroscopy are being developed for applications in several areas including biomedical analysis,[2,3] nucleic acid diagnostics,[4,5] and detection of biohazard materials and organisms.[6,7] Moreover, the control and manipulation of the SP surface propagation is being achieved for the full development of "plasmonic" circuits and devices that operate in the sub-wavelength range.[8,9] SPs are surface-bound electromagnetic waves, and so their characteristics depend heavily on the optical properties of materials at the metal−analyte interface.[1] This inherent dependence on local refractive index changes is the physical basis for the high sensitivity found in commercially available surface plasmon resonance (SPR) sensors that operate in the Kretschmann configuration.[3,10] Sensors based on changes in the maximum of the SP absorption due to the adsorption of organic molecules on ultrathin gold island films are also being developed using transmission mode (T-SPR).[11]

Another important consequence of the surface-confined characteristics of the SP waves is field localization;[12] the electromagnetic fields in structures that support SP modes are concentrated in nanoscopic regions smaller than the free wavelength of the excitation radiation. The resulting large localized field density allows the observation of an enhanced spectroscopic response from molecular species adsorbed at the

† Department of Chemistry, University of Victoria.
‡ Department of Electrical and Computer Engineering, University of Victoria.
§ Simon Fraser University.

(1) Raether, H. *Surface Plasmons on Smooth and Rough Surfaces and on Gratings*; Springer: Toronto, 1988.
(2) Haes, A. J.; Hall, W. P.; Chang, L.; Klein, W. L.; Van Duyne, R. P. *Nano Lett.* **2004**, *4*, 1029−1034.
(3) Nice, E. C.; Catimel, B. *BioEssays* **1999**, *21*, 339−352.
(4) Storhoff, J. J.; Lucas, A. D.; Garimella, V.; Bao, Y. P.; Muller, U. R. *Nat. Biotechnol.* **2004**, *22*, 883−887.
(5) Cao, Y. C.; Jin, R.; Mirkin, C. A. *Science* **2002**, *297*, 1536−1540.
(6) Zhang, X. Y.; Young, M. A.; Lyandres, O.; Van Duyne, R. P. *J. Am. Chem. Soc.* **2005**, *127*, 4484−4489.
(7) Marla, S.; Bao, P.; Mehta, H.; Hagenow, S.; Storhoff, J.; Garimella, V.; Lucas, A.; Muller, U. *Abstr. Pap.-Am. Chem. Soc.* **2003**, *225*, U109−U109.
(8) Barnes, W. L.; Dereux, A.; Ebbesen, T. W. *Nature* **2003**, *424*, 824−830.
(9) Hohenau, A.; Krenn, J. R.; Stepanov, A. L.; Drezet, A.; Ditlbacher, H.; Steinberger, B.; Leitner, A.; Aussenegg, F. R. *Opt. Lett.* **2005**, *30*, 893−895.
(10) Homola, J.; Yee, S. S.; Gauglitz, G. *Sens. Actuators, B* **1999**, *54*, 3−15.
(11) Kalyuzhny, G.; Vaskevich, A.; Schneeweiss, M. A.; Rubinstein, I. *Chem.-Eur. J.* **2002**, *8*, 3850−3857.
(12) Hutter, E.; Fendler, J. H. *Adv. Mater.* **2004**, *16*, 1685−1706.

10.1021/ja0548687 CCC: $30.25

nanostructures.[12,13] This phenomenon is the principle for a set of linear and nonlinear enhanced spectroscopic methods, including surface-enhanced Raman scattering (SERS),[13,14] surface-enhanced fluorescence spectroscopy (SEFS),[15−17] surface-enhanced infrared spectroscopy (SEIRS),[18] and surface-enhanced second-harmonic generation (SESHG).[19,20]

Colloidal nanoparticles,[13] arrays of clusters,[2] and roughened electrode surfaces[14] are among the typical nanostructured metallic substrates used for surface-enhanced spectroscopic methods. However, for analytical applications, the utilization of highly ordered structures, including metallic gratings, could offer a number of potential advantages, including greater reproducibility, higher sensitivity, and more convenient experimental geometries. Recently, metallic transmission gratings were shown to support SP excitation, leading to an extraordinary increase in the amount of light transmitted through the grating at specific wavelengths.[21] These gratings consisted of regular arrays (generally rectangular) of sub-wavelength holes milled in gold thin films. Because SPs are involved in this enhanced transmission, it was expected that such arrays could also present surface sensitivity to molecular adsorption and thus support enhanced spectroscopy. These properties were demonstrated recently by our group[22,23] and others.[24−31] Arrays of nanoholes in gold films were used as refractive index sensors, showing monolayer sensitivity to the adsorption of organic films and proteins.[22] We have also shown that the arrays can support SERS, with an enhancement factor that is dependent on the periodicity (i.e., distances between the holes) of the arrays.[23]

In this paper, we will extend the range of analytical applications of these substrates by showing that the SP-enhanced transmission can also be used for fluorescence detection. An enhancement in fluorescence through arrays of nanoholes has been previously demonstrated.[24−26] A fixed excitation wavelength was used, and the enhancement factor was tuned by rotating the arrays to achieve the Bragg resonance condition. The method was used to demonstrate an affinity biosensor platform for real-time detection of oligonucleotides.[25] Although that scheme presents the obvious advantage that detection can be achieved using a fixed laser source, the moving stage could be a problem for device implementation and miniaturization, because it may require precise optical alignment and moving parts (such as a rotation stage) with the associated controls and electronics. A completely different approach is to tune the SP resonance by changing the spacing between the nanoholes, to maximize the fluorescence from a specific dye; the potential of this strategy is demonstrated in the present work. We will demonstrate that the fluorescence of an oxazine dye is maximized for arrays of nanoholes with specific geometrical parameters, which is the first step toward the design of detection schemes based on this type of substrate. The enhanced fluorescence is accompanied by an increase in the sensitivity (defined as change in emission by change in concentration) when the SP resonance is achieved. Finally, we will show that this approach allows the detection of the analytical fluorescence signal in transmission mode at normal incidence, which is much more convenient than other geometries in terms of optical alignment and fabrication.[22]

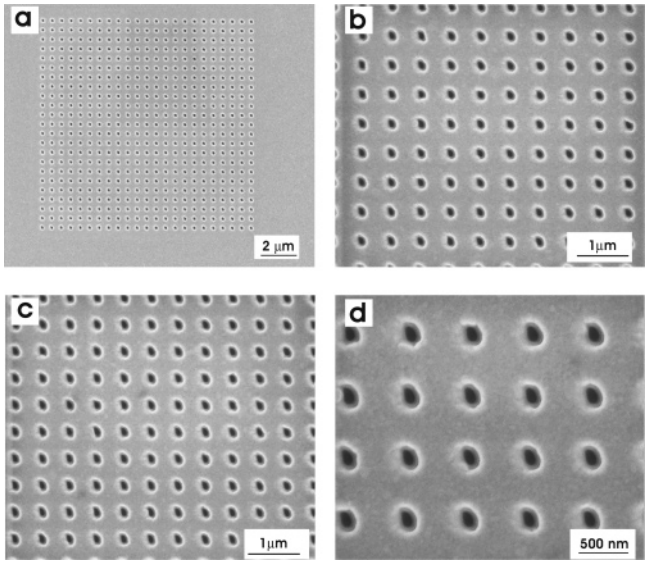

Figure 1. Scanning electron microscope (SEM) images of typical arrays of nanoholes obtained at different magnifications. (a) and (b) $p = 431$ nm; (c) and (d) $p = 500$ nm.

Experimental Section

The arrays of sub-wavelength holes in Au films were fabricated and imaged using a FEI 235 dualbeam focused ion beam (FIB) and field-emission scanning electron microscope. The details of the instrument setting, fabrication, cleaning, and optical characterization of the arrays are presented elsewhere.[22,23,32] The geometrical parameters of the arrays prepared using the FIB technique can be easily reproduced within 5 nm. Seven different square arrays with distinct periodicities were fabricated. Figure 1 shows scanning electron microscopy (SEM) images of typical arrays of nanoholes used in this work.

The arrays were constructed with the following periodicities: 353, 407, 431, 500, 553, 613, and 653 nm, with an average nanohole diameter of 100 nm for all arrays. The arrays were created in 100 nm-thick gold films deposited on Cr-coated (5 nm) glass by evaporation (from evaporated metal films (EMF)).

(13) Kneipp, K.; Kneipp, H.; Itzkan, I.; Dasari, R. R.; Feld, M. S. *Chem. Rev.* **1999**, *99*, 2957−2975.
(14) Brolo, A. G.; Irish, D. E.; Smith, B. D. *J. Mol. Struct.* **1997**, *405*, 29−44.
(15) Yu, F.; Persson, B.; Lofas, S.; Knoll, W. *J. Am. Chem. Soc.* **2004**, *126*, 8902−8903.
(16) Yu, F.; Tian, S. J.; Yao, D. F.; Knoll, W. *Anal. Chem.* **2004**, *76*, 3530−3535.
(17) Aroca, R.; Kovacs, G. J.; Jennings, C. A.; Loutfy, R. O.; Vincett, P. S. *Langmuir* **1988**, *4*, 518−521.
(18) Aroca, R. F.; Ross, D. J.; Domingo, C. *Appl. Spectrosc.* **2004**, *58*, 324a−338a.
(19) Chen, C. K.; Decastro, A. R. B.; Shen, Y. R. *Phys. Rev. Lett.* **1981**, *46*, 145−148.
(20) Brolo, A. G.; Germain, P.; Hager, G. *J. Phys. Chem. B* **2002**, *106*, 5982−5987.
(21) Ebbesen, T. W.; Lezec, H. J.; Ghaemi, H. F.; Thio, T.; Wolff, P. A. *Nature* **1998**, *391*, 667−669.
(22) Brolo, A. G.; Gordon, R.; Leathem, B.; Kavanagh, K. L. *Langmuir* **2004**, *20*, 4813−4815.
(23) Brolo, A. G.; Arctander, E.; Gordon, R.; Leathem, B.; Kavanagh, K. L. *Nano Lett.* **2004**, *4*, 2015−2018.
(24) Liu, Y.; Blair, S. *Opt. Lett.* **2003**, *28*, 507−509.
(25) Liu, Y.; Bishop, J.; Willians, L.; Blair, S.; Herron, J. *Nanotechnology* **2004**, *15*, 1368−1374.
(26) Liu, Y.; Blair, S. *Opt. Express* **2004**, *12*, 3686−3693.
(27) Nahata, A.; Linke, R. A.; Ishi, T.; Ohashi, K. *Opt. Lett.* **2003**, *28*, 423−425.
(28) Rodriguez, K. R.; Shah, S.; Williams, S. M.; Teeters-Kennedy, S.; Coe, J. V. *J. Chem. Phys.* **2004**, *121*, 8671−8675.
(29) Williams, S. M.; Rodriguez, K. R.; Teeters-Kennedy, S.; Shah, S.; Rogers, T. M.; Stafford, A. D.; Coe, J. V. *Nanotechnology* **2004**, *15*, S495−S503.
(30) Williams, S. M.; Rodriguez, K. R.; Teeters-Kennedy, S.; Stafford, A. D.; Bishop, S. R.; Lincoln, U. K.; Coe, J. V. *J. Phys. Chem. B* **2004**, *108*, 11833−11837.
(31) Willians, S. M.; Stafford, A. D.; Rodriguez, K. R.; Rogers, T. M.; Coe, J. V. *J. Phys. Chem. B* **2003**, *107*, 11871−11879.
(32) Gordon, R.; Brolo, A. G.; McKinnon, A.; Rajora, A.; Leathem, B.; Kavanagh, K. L. *Phys. Rev. Lett.* **2004**, *92*, 037401.

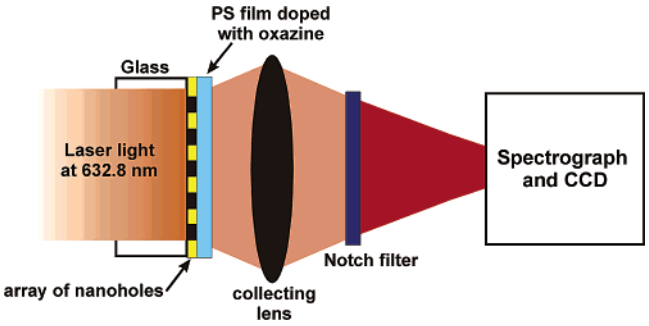

Figure 2. Schematic representation of the experimental setup for fluorescence measurements in transmission mode.

The clean gold surface of the nanohole arrays was modified by polystyrene (PS) films doped with oxazine 720 (Lambdachrome). The films were spin-coated at 2000 rpm from a 2% (w/w) solution of polystyrene in toluene doped with the desired concentration of the dye (ranging from 3 to 10 μM). The solvent was allowed to evaporate, resulting in a homogeneous film of oxazine dispersed in PS covering the arrays of nanoholes. Notice that, because the toluene evaporates away during the casting process, the actual concentration of the dye in the film is ~50 times larger than the original concentration in the solution. Fluorescence intensities obtained from films on the arrays and on glass were found to be linear with dye concentration within the film, indicating that auto-absorption effects were not significant in the range of concentrations investigated and that reproducible film thicknesses were obtained in all cases.

The arrays were optically characterized using an Olympus BHSM metallurgical microscope coupled to an Ocean Optics USB-2000 miniature fiber optic spectrometer as shown elsewhere.[22] All transmission measurements were done in a collinear geometry using a 100× objective lens (NA = 1.25). The halogen lamp from the microscope was the light source for the transmission measurements; the acquisition time was 200 ms, and 20 accumulations were recorded. The fluorescence measurements were also done in transmission mode (instead of the conventional 90° arrangement), with a 35 mW He−Ne laser (Melles Griot) as the excitation source (excitation wavelength of 632.8 nm), as shown in Figure 2.

The laser was directed from the glass side of the substrate and focused onto the array of nanoholes using a 10× Olympus microscope objective (numerical aperture = 0.25). The light transmitted through the nanoholes excited the fluorescence from the PS/oxazine films on the opposite side of the gold substrate (see Figure 2) and was collected using a similar microscope lens. This experimental geometry guarantees that the excitation travels through the nanoholes before impinging on the gold−film interface, allowing the excitation to be tuned via the SP resonances. The same setup was used to detect fluorescence from films on glass substrates without the nanohole arrays. The fundamental laser line from the transmitted light was rejected using a Kaiser super-notch filter, and the remaining radiation was directed through a Kaiser Holospec f/1.4 spectrograph coupled with an Andor CCD detector (model DV-401-BV). The substrates and the lenses were mounted on mechanical stages that allowed fine positioning control, while a wide-view microscope was used to aid the alignment of the incoming laser light with the ca. 16 μm × 16 μm arrays of nanoholes.

Results and Discussion

The arrays of nanoholes support enhanced transmission at certain wavelengths that match the SP resonance condition. For normal incidence, the SP resonance (λ_{SP}) can be calculated using:[21]

$$\lambda^{SP}(i,j) = p(i^2 + j^2)^{-1/2}\left(\frac{\epsilon_d \epsilon_m}{\epsilon_d + \epsilon_m}\right)^{1/2} \qquad (1)$$

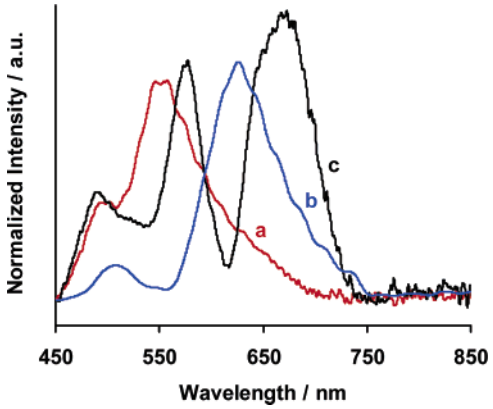

Figure 3. Transmission spectra of white light through arrays of nanoholes. (a) Uncoated array with p = 440 nm; (b) uncoated array with p = 550 nm; (c) same array as in (a) (p = 440 nm), but coated with a PS film doped with 3 μM oxazine 720 dye.

where p is the periodicity of the array, ϵ_m and ϵ_d are the dielectric constants of the metal and the dielectric material in contact with the metallic surface, respectively, and i and j are integers that define the scattering orders of the array. Although eq 1 is not exact,[33,34] it provides the essential features of the physics of SP resonance for applications in analytical devices. For instance, it is clear from eq 1 that the SP resonances of arrays in a given metal depend on the dielectric properties of the interface and on the distance between the holes (periodicity).

These dependences are readily visualized in Figure 3, where the effects of the periodicity and the refractive index of the interface are demonstrated. Each transmission spectra present characteristic SP resonance peaks that can be assigned using eq 1. The effect of the periodicity p on the SP resonance is illustrated by comparing the transmission spectra (a) and (b) in Figure 3. The resonance at 550 nm in spectrum (a) is assigned, according to eq 1, to a (1,0) resonance of the array with periodicity p = 440 nm. This resonance shifts to 623 nm in spectrum (b) due to an increase in the distance between the holes in the array with p = 550 nm. The change in the dielectric constant of the medium in contact with the metallic surface also has a prominent effect on the position of the SP resonances, as illustrated by comparing spectra (a) and (c); both spectra were obtained from the same array of nanoholes with p = 440 nm, with (a) being the spectrum from the uncoated array and (b) being the spectrum from the array coated with a PS/oxazine film (refractive index ca. 1.46). We note that the very small quantities of dye within the films do not significantly affect the refractive index, and so the shift in SP resonance is similar for arrays coated with PS films containing all dye concentrations investigated. In contrast to (a), spectrum (c) shows two resonances within the wavelength range presented; the peak at 670 nm is again a (1,0) SP resonance observed at 550 nm in (a), but this resonance is now shifted to longer wavelength. The shift in the (1,0) SP resonance observed by comparing spectra (a) and (c) is predicted according to eq 1. The other peak observed in (c), at 570 nm, is related to the (1,1) SP mode, which is another SP resonance order that moved into the experimental spectral window as the refractive index at the

(33) Enoch, S.; Popov, E.; Neviere, M.; Reinisch, R. *J. Opt. A: Pure Appl. Opt.* **2002**, *4*, S83−S87.
(34) Genet, C.; Exter, M. P. v.; Woerdman, J. P. *Opt. Commun.* **2003**, *225*, 331−336.

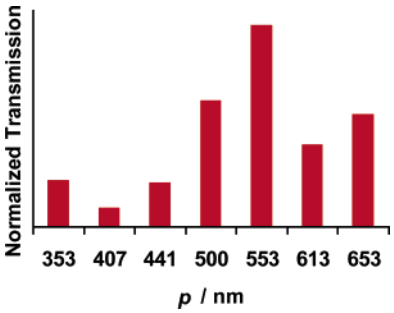

Figure 4. Normalized transmission of white light at 632.8 nm for arrays of nanoholes with different periodicities (p), each coated with a PS film doped with 3 μM oxazine 720 dye.

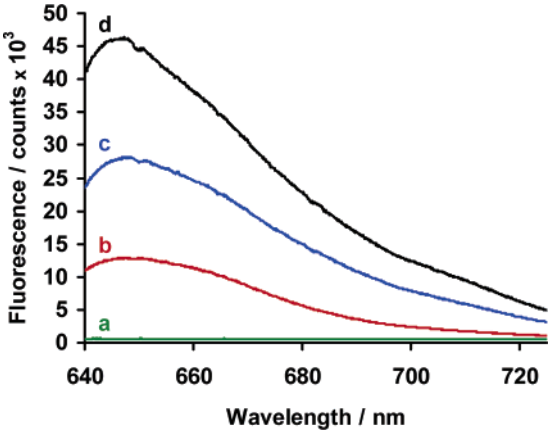

Figure 5. (a) Background fluorescence emission from an array of nanoholes with $p = 553$ nm coated with a PS film in the absence of oxazine 720; (b) emission from an array of nanoholes with $p = 407$ nm coated with a PS film doped with 3 μM of oxazine 720; (c) emission from an array of nanoholes with $p = 653$ nm coated with a PS film doped with 3 μM of oxazine 720; (d) emission from an array of nanoholes with $p = 553$ nm coated with a PS film doped with 3 μM of oxazine 720.

interface was increased. All other arrays were characterized as in Figure 3 by obtaining the transmission spectra in the presence and absence of the PS/oxazine films.

As shown in Figure 2, the fluorescence measurements were carried out using 632.8 nm excitation, with the laser light being transmitted through the nanoholes from the glass side of the array; the transmitted light then excited the dye molecules in the PS film on the opposite side of the array. The fluorescence intensity, which is directly related to the intensity of the excitation source, should therefore be correlated with the transmission at 632.8 nm for each array. The normalized transmission at 632.8 nm, obtained from the white light transmission measurements for coated arrays with different periodicities, is shown in Figure 4. Figure 4 indicates that more laser light (and therefore excitation) is expected to be transmitted through the arrays when the periodicities are between 500 and 550 nm.

Figure 5 shows the oxazine fluorescence emission obtained for three different arrays of nanoholes, each coated with PS films doped with 3 μM of the fluorescent dye. Spectrum (a) is a background run using the array with $p = 553$ nm coated with a pure PS film in the absence of the dye. Spectra (b), (c), and (d) are from arrays with $p = 407$, 653, and 553 nm, respectively, each coated with a PS film doped with 3 μM oxazine 720. Comparison of these spectra clearly indicates that the intensity of the fluorescence emission is array-dependent. The most

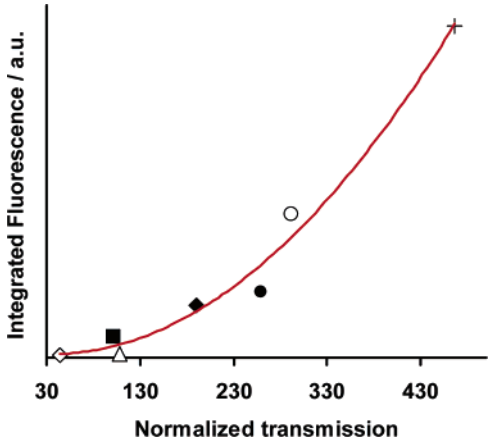

Figure 6. Relationship between the integrated fluorescence (background subtracted) and the normalized transmission at 632.8 nm. Each point corresponds to a different array of nanoholes. The periodicities were: (△) 353 nm; (◇) 407 nm; (■) 441 nm; (○) 500 nm; (+) 553 nm; (◆) 613 nm, (●) 653 nm.

intense fluorescence was obtained from the array ($p = 553$) that exhibited the greatest transmission of the excitation light (Figure 4), and the least intense fluorescence was obtained from the array ($p = 407$) showing the smallest amount of transmitted excitation light.

The fluorescence intensities for each of the arrays investigated (including the spectra shown in Figure 5) were background corrected and integrated. The correlation between the integrated fluorescence and the amount of transmission at 632.8 nm (shown Figure 4) is plotted in Figure 6. It is clear from Figure 6 that the relationship is nonlinear and as the energy of the excitation approaches the SP resonance condition of the array the amount of fluorescence increases rapidly. This nonlinearity cannot be explained simply in terms of the enhanced excitation, because the emission should only increase linearly with the normalized transmission at 632.8 nm. It is possible that the nonlinearity arises from a secondary enhancement effect from the oxazine emission, because the emission is also matched to the SP resonance for these wavelengths (see Figures 3 and 5). Such a combined effect would resemble the multiplicative enhancement observed in SERS.[35] In SERS, the Raman emitted field also excites the SP of the nanostructure, providing an additional contribution to the overall effect. Reports of a double-enhancement in surface enhanced fluorescence are less common, and more experiments are required to substantiate this proposed mechanism. It is important to point out that, due to the geometry of the experiment (shown in Figure 2), the resonance with the excitation is essential for the production of large amounts of emission. Therefore, a hypothetical situation where only the emission is resonant with the SPs would yield an amount of fluorescence limited by the transmission of the excitation. On the other hand, although the excitation wavelength, at 632.8 nm, is above the cutoff condition for transmission through a 100 nm hole,[36] a small amount of radiation is still evanescently transmitted even in a nonresonant situation. It is therefore expected that a residual amount of fluorescence emission from the film should be observed even in nonresonant conditions with the excitation energy.

(35) Schatz, G. C.; Duyne, R. P. V. In *Handbook of Vibrational Spectroscopy*; Griffiths, P. R., Ed.; Wiley: Chichester, 2002.
(36) Gordon, R.; Brolo, A. G. *Opt. Express* **2005**, *13*, 1933−1938.

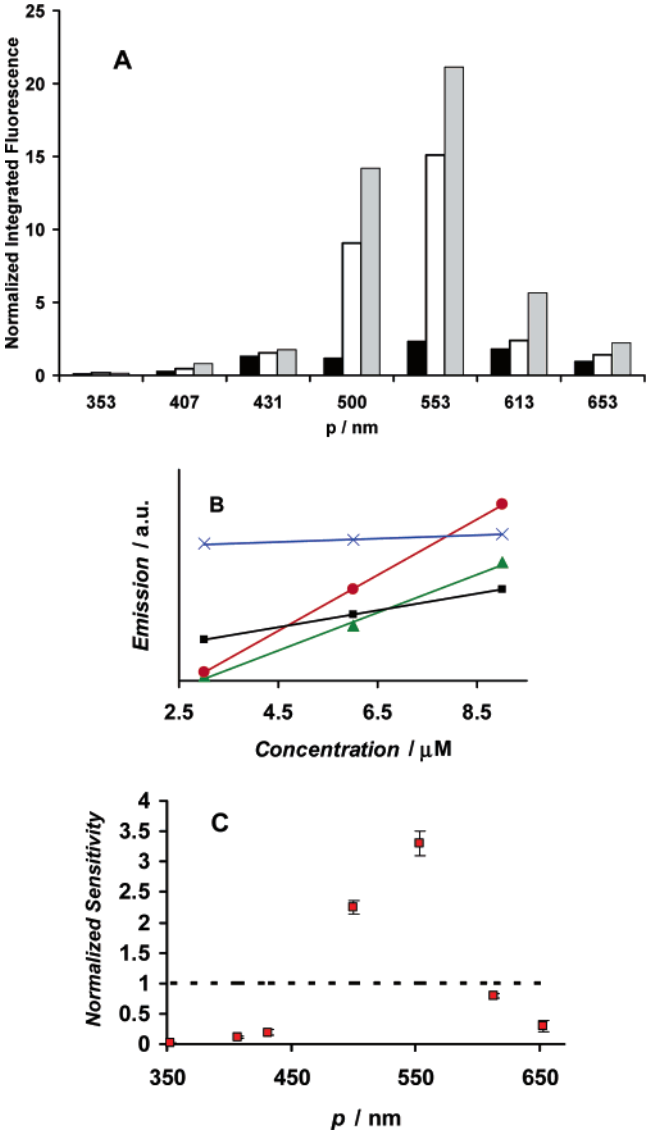

Figure 7. (A) Integrated fluorescence emission from arrays of nanoholes coated with PS films doped with different concentrations of oxazine 720. Black [oxazine 720] = 3.2 μM; white [oxazine 720] = 5.8 μM; gray [oxazine 720] = 9.1 μM. (B) Integrated emission versus oxazine concentration plots. (■) PS-doped film on glass slides; (×) PS-doped film on an array of nanoholes with p = 431 nm; (▲) PS-doped film on an array of nanoholes with p = 500 nm; (●) PS-doped film on an array of nanoholes with p = 553 nm. The emission values were offset for better visualization. (C) Sensitivity from oxazine films on arrays with different periodicities (p) normalized by the sensitivity obtained from oxazine-covered glass slides. The dashed horizontal line at S = 1 corresponds to the sensitivity of the film-coated glass slide. The error bars indicate that the spread in the determination of S was between 5% and 25%, with larger relative deviations observed for the cases where S < 1.

Figure 7 shows the integrated emission from the various arrays coated with PS films containing different concentrations of oxazine 720. Figure 7 indicates that not only the total amount of fluorescence emission, but also the sensitivity (signal increase with increase in concentration) of the device is improved as the SP resonance is approached. The sensitivity (S) is proportional to the intensity of the excitation (I_0), according to: $S = kI_0$, where k is the proportionality constant. The S values were obtained from the slopes of emission versus concentration of oxazine 720; some of these plots are shown in Figure 7B, and it is easily observable that the slopes obtained from the arrays are different from the one obtained from the film-coated glass

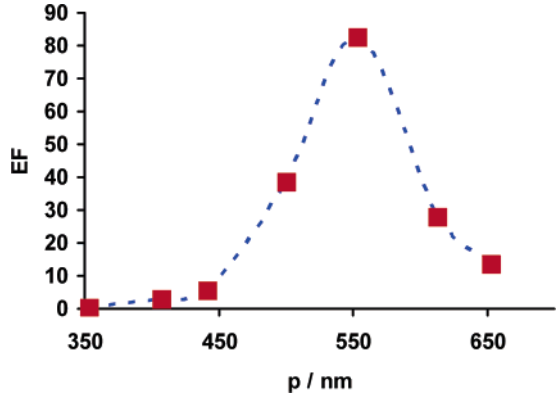

Figure 8. Calculated enhancement factor (EF) for arrays of nanoholes with different periodicities. Arrays of nanoholes were coated with a PS film doped with 9.6 μM oxazine 720.

slide. To quantify the change in sensitivity induced by the arrays, the S values obtained for each array were normalized by the sensitivity measured using glass slides. The normalized sensitivity is smaller than 1 for the off-resonance condition. However, the normalized sensitivity increases by roughly 3 times when the best resonance condition for these arrays is attained (see Figure 7C). Good reproducibility of the fluorescence data was obtained once the film deposition procedure and concentration range were optimized, as can be seen from the small error bars shown in Figure 7C.

Finally, the SP-mediated enhancement of the fluorescence was also estimated for each array. This was done by integrating the emission from each film-coated array and dividing these values by the integrated fluorescence obtained from glass slides coated with a PS film prepared using the same procedure. The ratio was then normalized by the fill factor of the arrays (area fraction of holes in the array).[24,25] This normalization was also performed in the data presented in Figure 7. This correction is required because most of the area illuminated in the array experiments is not transparent to the excitation. The Bethe's law correction,[37] which takes into account the fact that the excitation beam is above cutoff and cannot propagate into the opening, was not considered.[21] The calculated enhancement factors (EF) are presented in Figure 8.

The EF is dependent on the geometric properties of the arrays and maximizes for p = 553 nm. The maximum value for EF found in this work was 82. This value agrees well with previous EF obtained using arrays of nanoholes. For instance, Liu and Blair reported an enhancement of 40 times on the fluorescence from a monolayer of egg white avidin labeled with Cy-5 dye when the conditions for maximum transmission of the excitation light were satisfied.[24] Figure 8 shows that it is possible to selectively enhance the fluorescence emission of specific dyes by tailoring the geometrical characteristics of the array. This approach is suitable for miniaturization, although the requirement of different excitations to detect specific dyes is a limitation of the method. This limitation can be overcome in the future by either using a combination of broad light excitation and filters or using a set of miniaturized laser diodes. Another limitation is the serial characteristic of the FIB method, although this problem should be overcome as soon as new methods for efficient parallel fabrication of arrays of nanoholes became

(37) Bethe, H. A. *Phys. Rev.* **1944**, *66*, 163−182.

available in the literature. It is also important to point out that the local field effect responsible for the enhancement (SP excitation) is distance dependent and maximizes at the surface.[1] On the other hand, the photoluminescence from organic fluorophores is known to be quenched when the emitter is in the proximity of a metallic substrate.[38] The distance dependence of fluorescence for emitters within the local resonant SP-field has been demonstrated by several authors in a variety of systems[39,40] and is consistently found to reach a maximum for fluorophores located within ~10 nm from the metallic surface. In our system, the oxazine dye molecules, or aggregates of molecules, are believed to be dispersed randomly throughout the film, trapped in the PS matrix by fast evaporation of solvent during spin-coating, with a distribution of distances from the metal surface. It is then possible to further optimize the analytical method by selectively placing the fluorophores at a certain distance from the array of nanoholes using an appropriated spacer. This should not result in a decrease in the amount of emission, but would prevent quenching effects for fluorophores in proximity to the metal, and the photodecomposition of fluorophores exposed to the highest field near the surface.

Conclusions

In summary, this paper demonstrates that arrays of nanoholes can be used to fabricate analytical devices for enhanced fluorescence measurements, with fluorescence enhancement via SP resonance being tunable via the periodicity of the array. By tuning the transmission and localization of laser excitation using different geometric parameters of the arrays, it is possible to obtain a significant increase in the amount of fluorescence relative to that obtained from identical films coated onto glass slides (after the fill factor correction). The observed increase in fluorescence with increasing concentration (sensitivity) was also enhanced when the SP resonance condition is achieved. These results suggest that arrays of nanoholes in Au films at resonance can improve both the sensitivity and the limit of detection of fluorescence-based analysis. Moreover, these substrates should allow the confinement of the analyte in nanometric regions (i.e., within the nanoholes). This combination of spatial confinement and enhanced spectroscopic response could lead to the development of a new generation of devices for ultra-sensitive analysis of minute amounts of biological and nonbiological analytes. The collinear geometry of our optical measurements is also more suitable for miniaturization than other types of SPR devices that operate in reflection mode.

Acknowledgment. We gratefully acknowledge funding support for this work from NSERC, CFI, and BCKDF. This collaboration has also been facilitated by the Centre for Advanced Materials and Related Technology (CAMTEC) at the University of Victoria and by the Pacific Centre for Advanced Materials and Microstructures (PCAMM).

JA0548687

(38) Ritchie, G.; Burstein, E. *Phys. Rev. B* **1981**, *24*, 4843−4846.
(39) Kulakovich, O.; Strekal, N.; Yaroshevich, A.; Maskevich, S.; Gaponenko, S.; Nabiev, I.; Woggon, U.; Artemyev, M. *Nano Lett.* **2002**, *2*, 1449−1452.
(40) Dulkeith, E.; Ringler, M.; Klar, T. A.; Feldmann, J.; Javier, A. M.; Parak, W. J. *Nano Lett.* **2005**, *5*, 585−589.